Wavelet Methods for Time Series Analysis

Part III: MODWT and Examples of DWT/MODWT Analysis

- MODWT stands for 'maximal overlap discrete wavelet transform' (pronounced 'mod WT')
- transforms very similar to the MODWT have been studied in the literature under the following names:
  - undecimated DWT (or nondecimated DWT)
  - stationary DWT
  - translation (or time) invariant DWT
  - redundant DWT
- also related to notions of 'wavelet frames' and 'cycle spinning'
- basic idea: use values removed from DWT by downsampling

Quick Comparison of the MODWT to the DWT

- unlike the DWT, MODWT is not orthonormal (in fact MODWT is highly redundant)
- unlike the DWT, MODWT is defined naturally for all samples sizes (i.e., N need not be a multiple of a power of two)
- similar to the DWT, can form multiresolution analyses (MRAs) using MODWT, but with certain additional desirable features; e.g., unlike the DWT, MODWT-based MRA has details and smooths that shift along with $\mathbf{X}$ (if $\mathbf{X}$ has detail $\widetilde{\mathcal{D}}_j$, then $\mathcal{T}^m\mathbf{X}$ has detail $\mathcal{T}^m\widetilde{\mathcal{D}}_j$)
- similar to the DWT, an analysis of variance (ANOVA) can be based on MODWT wavelet coefficients
- unlike the DWT, MODWT discrete wavelet power spectrum same for $\mathbf{X}$ and its circular shifts $\mathcal{T}^m\mathbf{X}$

DWT Wavelet & Scaling Filters and Coefficients

- recall that we obtain level $j = 1$ DWT wavelet and scaling coefficients from $\mathbf{X}$ by filtering and downsampling:

$$\mathbf{X} \longrightarrow \boxed{H(\tfrac{k}{N})} \underset{\downarrow 2}{\longrightarrow} \mathbf{W}_1 \text{ and } \mathbf{X} \longrightarrow \boxed{G(\tfrac{k}{N})} \underset{\downarrow 2}{\longrightarrow} \mathbf{V}_1$$

- transfer functions $H(\cdot)$ and $G(\cdot)$ are associated with impulse response sequences $\{h_l\}$ and $\{g_l\}$ via the usual relationships

$$\{h_l\} \longleftrightarrow H(\cdot) \text{ and } \{g_l\} \longleftrightarrow G(\cdot)$$

Level j Equivalent Wavelet & Scaling Filters

- for any level j, rather than using the pyramid algorithm, we could get the DWT wavelet and scaling coefficients directly from $\mathbf{X}$ by filtering and downsampling:

$$\mathbf{X} \longrightarrow \boxed{H_j(\tfrac{k}{N})} \underset{\downarrow 2^j}{\longrightarrow} \mathbf{W}_j \text{ and } \mathbf{X} \longrightarrow \boxed{G_j(\tfrac{k}{N})} \underset{\downarrow 2^j}{\longrightarrow} \mathbf{V}_j$$

- transfer functions $H_j(\cdot)$ & $G_j(\cdot)$ depend just on $H(\cdot)$ & $G(\cdot)$
  - actually can say 'just on $H(\cdot)$' since $G(\cdot)$ depends on $H(\cdot)$
  - note that $H_1(\cdot)$ & $G_1(\cdot)$ are the same as $H(\cdot)$ & $G(\cdot)$)
- impulse response sequences $\{h_{j,l}\}$ and $\{g_{j,l}\}$ are associated with transfer functions via the usual relationships

$$\{h_{j,l}\} \longleftrightarrow H_j(\cdot) \text{ and } \{g_{j,l}\} \longleftrightarrow G_j(\cdot),$$

and both filters have width $L_j = (2^j - 1)(L - 1) + 1$

Haar Equivalent Wavelet & Scaling Filters

- $L_j = 2^j$ is width of $\{h_{j,l}\}$ and $\{g_{j,l}\}$

D(4) Equivalent Wavelet & Scaling Filters

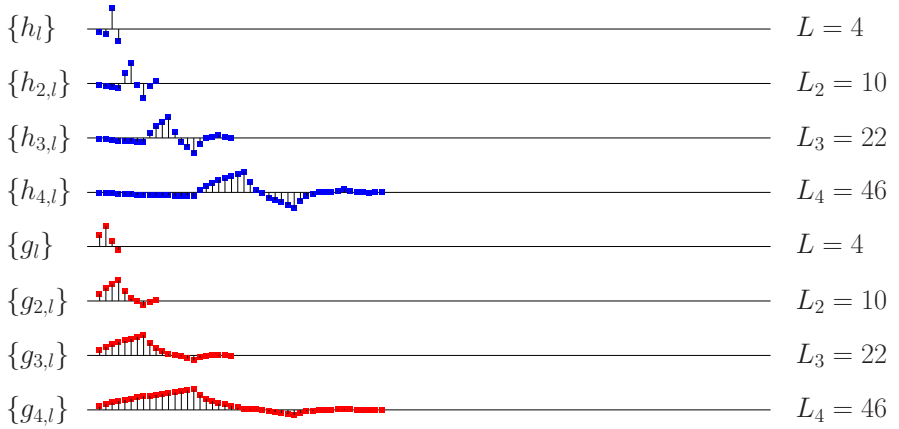

- L_j dictated by general formula $L_j = (2^j - 1)(L - 1) + 1$, but can argue that *effective* width is 2^j (same as Haar L_j)

D(6) Equivalent Wavelet & Scaling Filters

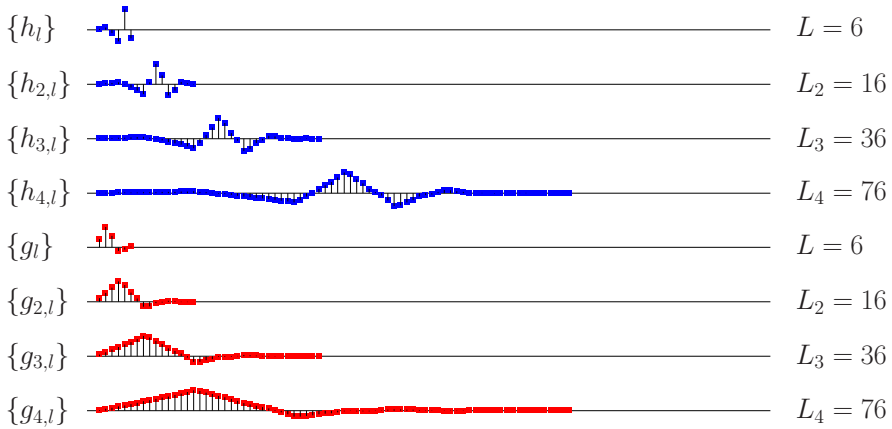

- $\{h_{4,l}\}$ resembles discretized version of Mexican hat wavelet

LA(8) Equivalent Wavelet & Scaling Filters

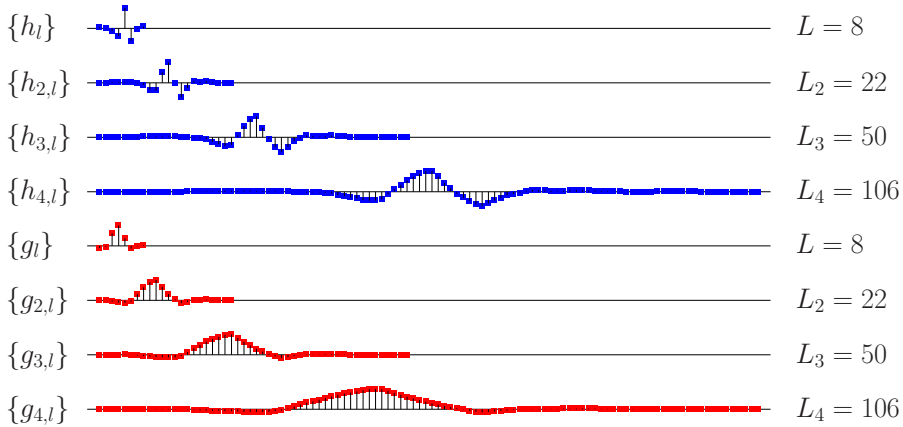

- $\{h_{j,l}\}$ resembles discretized version of Mexican hat wavelet, again with an effective width of 2^j

Squared Gain Functions for Equivalent Filters

- squared gain functions give us frequency domain properties:

$$\mathcal{H}_j(f) \equiv |H_j(f)|^2 \text{ and } \mathcal{G}_j(f) \equiv |G_j(f)|^2$$

- example: squared gain functions for LA(8) $J_0 = 4$ partial DWT

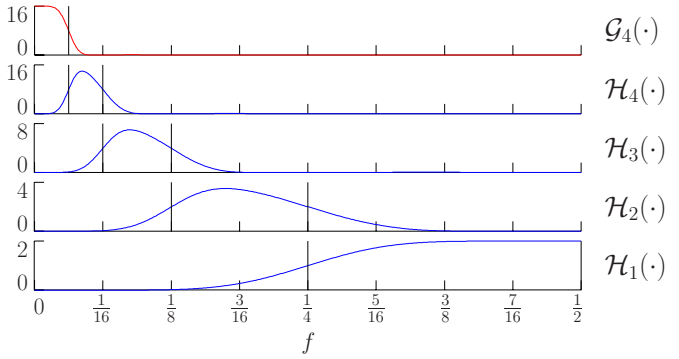

Definition of MODWT Wavelet & Scaling Filters

- define MODWT filters $\{\tilde{h}_{j,l}\}$ and $\{\tilde{g}_{j,l}\}$ by renormalizing the DWT filters (widths of MODWT & DWT filters are the same):

$$\tilde{h}_{j,l} = h_{j,l}/2^{j/2} \text{ and } \tilde{g}_{j,l} = g_{j,l}/2^{j/2}$$

- whereas DWT filters have unit energy, MODWT filters satisfy

$$\sum_{l=0}^{L_j-1} \tilde{h}_{j,l}^2 = \sum_{l=0}^{L_j-1} \tilde{g}_{j,l}^2 = \frac{1}{2^j}$$

- let $\widetilde{H}_j(\cdot)$ and $\widetilde{G}_j(\cdot)$ be the corresponding transfer functions:

$$\widetilde{H}_j(f) = \frac{1}{2^{j/2}} H_j(f) \text{ and } \widetilde{G}_j(f) = \frac{1}{2^{j/2}} G_j(f)$$

so that

$$\{\tilde{h}_{j,l}\} \longleftrightarrow \widetilde{H}_j(\cdot) \text{ and } \{\tilde{g}_{j,l}\} \longleftrightarrow \widetilde{G}_j(\cdot)$$

Definition of MODWT Coefficients: I

- level j MODWT wavelet and scaling coefficients are *defined* to be output obtaining by filtering $\mathbf{X}$ with $\{\tilde{h}_{j,l}\}$ and $\{\tilde{g}_{j,l}\}$:

$$\mathbf{X} \longrightarrow \boxed{\widetilde{H}_j(\tfrac{k}{N})} \longrightarrow \widetilde{\mathbf{W}}_j \text{ and } \mathbf{X} \longrightarrow \boxed{\widetilde{G}_j(\tfrac{k}{N})} \longrightarrow \widetilde{\mathbf{V}}_j$$

- compare the above to its DWT equivalent:

$$\mathbf{X} \longrightarrow \boxed{H_j(\tfrac{k}{N})} \underset{\downarrow 2^j}{\longrightarrow} \mathbf{W}_j \text{ and } \mathbf{X} \longrightarrow \boxed{G_j(\tfrac{k}{N})} \underset{\downarrow 2^j}{\longrightarrow} \mathbf{V}_j$$

- DWT and MODWT have different normalizations for filters, and there is no downsampling by 2^j in the MODWT
- level J_0 MODWT consists of $J_0 + 1$ vectors, namely,

$$\widetilde{\mathbf{W}}_1, \widetilde{\mathbf{W}}_2, \ldots, \widetilde{\mathbf{W}}_{J_0} \text{ and } \widetilde{\mathbf{V}}_{J_0},$$

each of which has length N

Definition of MODWT Coefficients: II

- MODWT of level J_0 has $(J_0+1)N$ coefficients, whereas DWT has N coefficients for any given J_0
- whereas DWT of level J_0 requires N to be integer multiple of 2^{J_0}, MODWT of level J_0 is well-defined for *any* sample size N
- when N is divisible by 2^{J_0}, we can write

$$W_{j,t} = \sum_{l=0}^{L_j-1} h_{j,l} X_{2^j(t+1)-1-l \bmod N} \text{ and } \widetilde{W}_{j,t} = \sum_{l=0}^{L_j-1} \tilde{h}_{j,l} X_{t-l \bmod N},$$

and we have the relationship

$$W_{j,t} = 2^{j/2} \widetilde{W}_{j,2^j(t+1)-1} \text{ and, likewise, } V_{J_0,t} = 2^{J_0/2} \widetilde{V}_{J_0,2^{J_0}(t+1)-1}$$

(here $\widetilde{W}_{j,t}$ & $\widetilde{V}_{J_0,t}$ denote the tth elements of $\widetilde{\mathbf{W}}_j$ & $\widetilde{\mathbf{V}}_{J_0}$)

Properties of the MODWT

- as was true with the DWT, we can use the MODWT to obtain
  - a scale-based additive decomposition (MRA) and
  - a scale-based energy decomposition (ANOVA)
- in addition, the MODWT can be computed efficiently via a pyramid algorithm

MODWT Multiresolution Analysis: I

- starting from the definition

$$\widetilde{W}_{j,t} = \sum_{l=0}^{L_j-1} \tilde{h}_{j,l} X_{t-l \bmod N}, \quad \text{can write} \quad \widetilde{W}_{j,t} = \sum_{l=0}^{N-1} \tilde{h}^{\circ}_{j,l} X_{t-l \bmod N},$$

  where $\{\tilde{h}^{\circ}_{j,l}\}$ is $\{\tilde{h}_{j,l}\}$ periodized to length N
- can express the above in matrix notation as $\widetilde{\mathbf{W}}_j = \widetilde{\mathcal{W}}_j \mathbf{X}$, where $\widetilde{\mathcal{W}}_j$ is the $N \times N$ matrix given by

$$\begin{bmatrix}
\tilde{h}^{\circ}_{j,0} & \tilde{h}^{\circ}_{j,N-1} & \tilde{h}^{\circ}_{j,N-2} & \tilde{h}^{\circ}_{j,N-3} & \cdots & \tilde{h}^{\circ}_{j,3} & \tilde{h}^{\circ}_{j,2} & \tilde{h}^{\circ}_{j,1} \\
\tilde{h}^{\circ}_{j,1} & \tilde{h}^{\circ}_{j,0} & \tilde{h}^{\circ}_{j,N-1} & \tilde{h}^{\circ}_{j,N-2} & \cdots & \tilde{h}^{\circ}_{j,4} & \tilde{h}^{\circ}_{j,3} & \tilde{h}^{\circ}_{j,2} \\
\vdots & \vdots & \vdots & \vdots & \cdots & \vdots & \vdots & \vdots \\
\tilde{h}^{\circ}_{j,N-2} & \tilde{h}^{\circ}_{j,N-3} & \tilde{h}^{\circ}_{j,N-4} & \tilde{h}^{\circ}_{j,N-5} & \cdots & \tilde{h}^{\circ}_{j,1} & \tilde{h}^{\circ}_{j,0} & \tilde{h}^{\circ}_{j,N-1} \\
\tilde{h}^{\circ}_{j,N-1} & \tilde{h}^{\circ}_{j,N-2} & \tilde{h}^{\circ}_{j,N-3} & \tilde{h}^{\circ}_{j,N-4} & \cdots & \tilde{h}^{\circ}_{j,2} & \tilde{h}^{\circ}_{j,1} & \tilde{h}^{\circ}_{j,0}
\end{bmatrix}$$

MODWT Multiresolution Analysis: II

- recalling the DWT relationship $\mathcal{D}_j = \mathcal{W}_j^T \mathbf{W}_j$, define jth level MODWT detail as $\widetilde{\mathcal{D}}_j = \widetilde{\mathcal{W}}_j^T \widetilde{\mathbf{W}}_j$
- similar development leads to definition for jth level MODWT smooth as $\widetilde{\mathcal{S}}_j = \widetilde{\mathcal{V}}_j^T \widetilde{\mathbf{V}}_j$
- can show that level J_0 MODWT-based MRA is given by

$$\mathbf{X} = \sum_{j=1}^{J_0} \widetilde{\mathcal{D}}_j + \widetilde{\mathcal{S}}_{J_0},$$

  which is analogous to the DWT-based MRA

MODWT Multiresolution Analysis: III

- if we form DWT-based MRAs for $\mathbf{X}$ and its circular shifts $\mathcal{T}^m \mathbf{X}$, $m = 1, \ldots, N-1$, we can obtain $\widetilde{\mathcal{D}}_j$ by appropriately averaging all N DWT-based details ('cycle spinning')

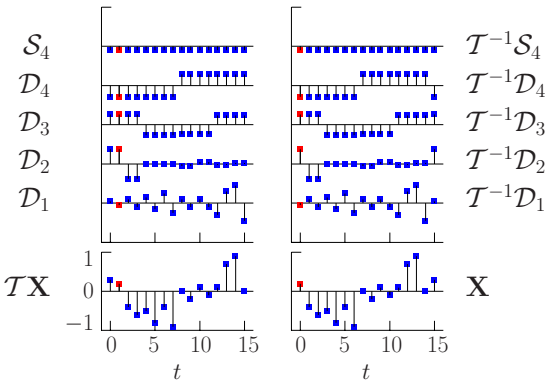

MODWT Multiresolution Analysis: IV

- left-hand plots show $\widetilde{\mathcal{D}}_j$, while right-hand plots show average of $\mathcal{T}^{-m}\mathcal{D}_j$ in MRA for $\mathcal{T}^m\mathbf{X}$, $m = 0, 1, \ldots, 15$

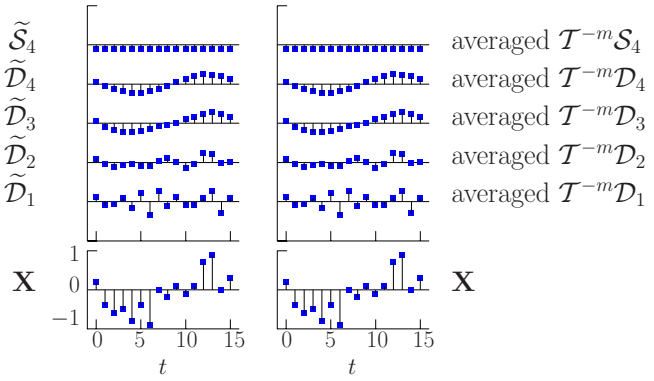

MODWT Decomposition of Energy

- for any $J_0 \geq 1$ & $N \geq 1$, can show that

$$\|\mathbf{X}\|^2 = \sum_{j=1}^{J_0} \|\widetilde{\mathbf{W}}_j\|^2 + \|\widetilde{\mathbf{V}}_{J_0}\|^2,$$

leading to an analysis of the sample variance of $\mathbf{X}$:

$$\hat{\sigma}_X^2 = \frac{1}{N}\sum_{j=1}^{J_0} \|\widetilde{\mathbf{W}}_j\|^2 + \frac{1}{N}\|\widetilde{\mathbf{V}}_{J_0}\|^2 - \overline{X}^2,$$

which is analogous to the DWT-based analysis of variance

MODWT Pyramid Algorithm

- goal: compute $\widetilde{\mathbf{W}}_j$ & $\widetilde{\mathbf{V}}_j$ using $\widetilde{\mathbf{V}}_{j-1}$ rather than $\mathbf{X}$
- letting $\widetilde{V}_{0,t} \equiv X_t$, can show that, for all $j \geq 1$,

$$\widetilde{W}_{j,t} = \sum_{l=0}^{L-1} \tilde{h}_l \widetilde{V}_{j-1,t-2^{j-1}l \bmod N} \quad \text{and} \quad \widetilde{V}_{j,t} = \sum_{l=0}^{L-1} \tilde{g}_l \widetilde{V}_{j-1,t-2^{j-1}l \bmod N}$$

- inverse pyramid algorithm is given by

$$\widetilde{V}_{j-1,t} = \sum_{l=0}^{L-1} \tilde{h}_l \widetilde{W}_{j,t+2^{j-1}l \bmod N} + \sum_{l=0}^{L-1} \tilde{g}_l \widetilde{V}_{j,t+2^{j-1}l \bmod N}$$

- algorithm requires $N \log_2(N)$ multiplications, which is the same as needed by fast Fourier transform algorithm

Example of $J_0 = 4$ LA(8) MODWT

- oxygen isotope records $\mathbf{X}$ from Antarctic ice core

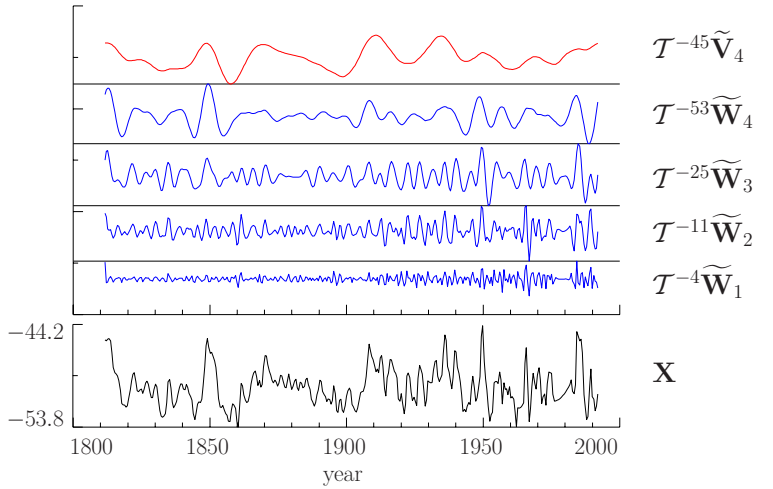

Relationship Between MODWT and DWT

- bottom plot shows $\mathbf{W}_4$ from DWT after circular shift $\mathcal{T}^{-3}$ to align coefficients properly in time
- top plot shows $\widetilde{\mathbf{W}}_4$ from MODWT and subsamples that, upon rescaling, yield $\mathbf{W}_4$ via $W_{4,t} = 4\widetilde{W}_{4,16(t+1)-1}$

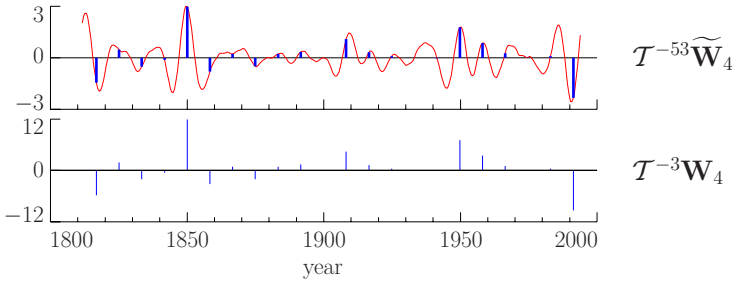

Example of $J_0 = 4$ LA(8) MODWT MRA

- oxygen isotope records $\mathbf{X}$ from Antarctic ice core

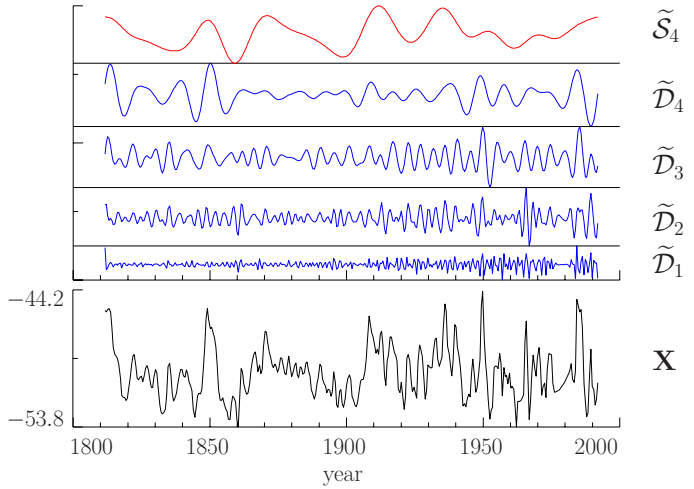

Example of Variance Decomposition

- decomposition of sample variance from MODWT

$$\hat{\sigma}_X^2 \equiv \frac{1}{N}\sum_{t=0}^{N-1}\left(X_t - \overline{X}\right)^2 = \sum_{j=1}^{4}\frac{1}{N}\|\widetilde{\mathbf{W}}_j\|^2 + \frac{1}{N}\|\widetilde{\mathbf{V}}_4\|^2 - \overline{X}^2$$

- LA(8)-based example for oxygen isotope records
  - 0.5 year changes: $\frac{1}{N}\|\widetilde{\mathbf{W}}_1\|^2 \doteq 0.145$ ($\doteq$ 4.5% of $\hat{\sigma}_X^2$)
  - 1.0 years changes: $\frac{1}{N}\|\widetilde{\mathbf{W}}_2\|^2 \doteq 0.500$ ($\doteq 15.6\%$)
  - 2.0 years changes: $\frac{1}{N}\|\widetilde{\mathbf{W}}_3\|^2 \doteq 0.751$ ($\doteq 23.4\%$)
  - 4.0 years changes: $\frac{1}{N}\|\widetilde{\mathbf{W}}_4\|^2 \doteq 0.839$ ($\doteq 26.2\%$)
  - 8.0 years averages: $\frac{1}{N}\|\widetilde{\mathbf{V}}_4\|^2 - \overline{X}^2 \doteq 0.969$ ($\doteq 30.2\%$)
  - sample variance: $\hat{\sigma}_X^2 \doteq 3.204$

Summary of Key Points about the MODWT

- similar to the DWT, the MODWT offers
  - a scale-based multiresolution analysis
  - a scale-based analysis of the sample variance
  - a pyramid algorithm for computing the transform efficiently
- unlike the DWT, the MODWT is
  - defined for all sample sizes (no 'power of 2' restrictions)
  - unaffected by circular shifts to $\mathbf{X}$ in that coefficients, details and smooths shift along with $\mathbf{X}$ (example coming later)
  - highly redundant in that a level J_0 transform consists of $(J_0 + 1)N$ values rather than just N
- as we shall see, the MODWT can eliminate 'alignment' artifacts, but its redundancies are problematic for some uses

Examples of DWT & MODWT Analysis: Overview

- look at DWT analysis of electrocardiogram (ECG) data
- discuss potential alignment problems with the DWT and how they are alleviated with the MODWT
- look at MODWT analysis of ECG data, subtidal sea level fluctuations, Nile River minima and ocean shear measurements
- discuss practical details
  - choice of wavelet filter and of level J_0
  - handling boundary conditions
  - handling sample sizes that are not multiples of a power of 2
  - definition of DWT not standardized

Electrocardiogram Data: I

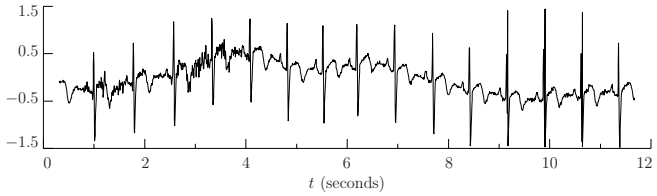

- ECG measurements $\mathbf{X}$ taken during normal sinus rhythm of a patient who occasionally experiences arhythmia (data courtesy of Gust Bardy and Per Reinhall, University of Washington)
- $N = 2048$ samples collected at rate of 180 samples/second; i.e., $\Delta t = 1/180$ second
- 11.38 seconds of data in all
- time of X_0 taken to be $t_0 = 0.31$ merely for plotting purposes

Electrocardiogram Data: II

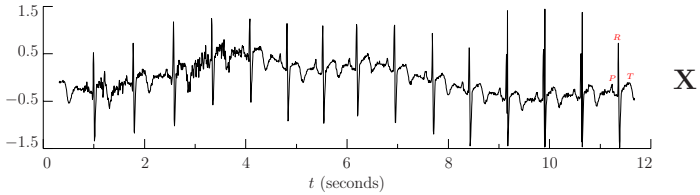

- features include
  - baseline drift (not directly related to heart)
  - intermittent high-frequency fluctuations (again, not directly related to heart)
  - 'PQRST' portion of normal heart rhythm
- provides useful illustration of wavelet analysis because there are identifiable features on several scales

Electrocardiogram Data: III

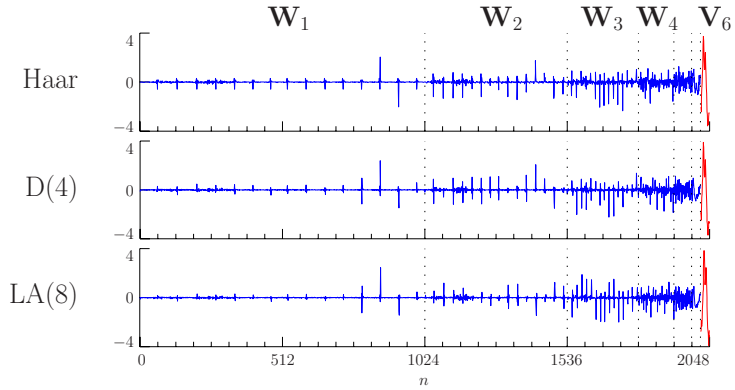

- partial DWT coefficients $\mathbf{W}$ of level $J_0 = 6$ for ECG time series using the Haar, D(4) and LA(8) wavelets (top to bottom)

Electrocardiogram Data: IV

- elements W_n of $\mathbf{W}$ are plotted versus $n = 0, \ldots, N-1 = 2047$
- vertical dotted lines delineate 7 subvectors $\mathbf{W}_1, \ldots, \mathbf{W}_6$ & $\mathbf{V}_6$
- sum of squares of 2048 coefficients $\mathbf{W}$ is equal to those of $\mathbf{X}$
- gross pattern of coefficients similar for all three wavelets

Electrocardiogram Data: V

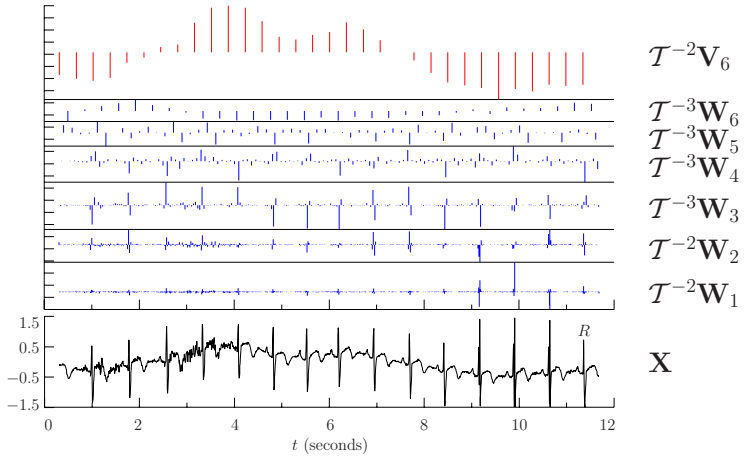

- LA(8) DWT coefficients stacked by scale and aligned with time
- spacing between major tick marks is the same in both plots

Electrocardiogram Data: VI

- R waves aligned with spikes in $\mathbf{W}_2$ and $\mathbf{W}_3$
- intermittent fluctuations appear mainly in $\mathbf{W}_1$ and $\mathbf{W}_2$
- setting $J_0 = 6$ results in $\mathbf{V}_6$ capturing baseline drift

Electrocardiogram Data: VII

- to quantify how well various DWTs summarize $\mathbf{X}$, can form normalized partial energy sequences (NPESs)
- given $\{U_t : t = 0, \ldots, N-1\}$, square and order such that

$$U^2_{(0)} \geq U^2_{(1)} \geq \cdots \geq U^2_{(N-2)} \geq U^2_{(N-1)}$$

- $U^2_{(0)}$ is largest of all the U^2_t values while $U^2_{(N-1)}$ is the smallest
- NPES for $\{U_t\}$ defined as

$$C_n \equiv \frac{\sum_{m=0}^{n} U^2_{(m)}}{\sum_{m=0}^{N-1} U^2_{(m)}}, \quad n = 0, 1, \ldots, N-1$$

Electrocardiogram Data: VIII

- plots show NPESs for
  - original time series (dashed curve, plot (a))
  - Haar DWT (solid curves, both plots)
  - D(4) DWT (dashed curve, plot (b)); LA(8) is virtually identical
  - DFT (dotted curve, plot (a)) with $|U_t|^2$ rather than U_t^2

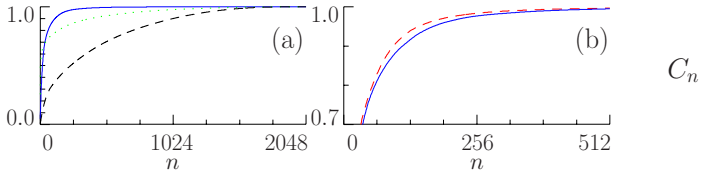

Electrocardiogram Data: IX

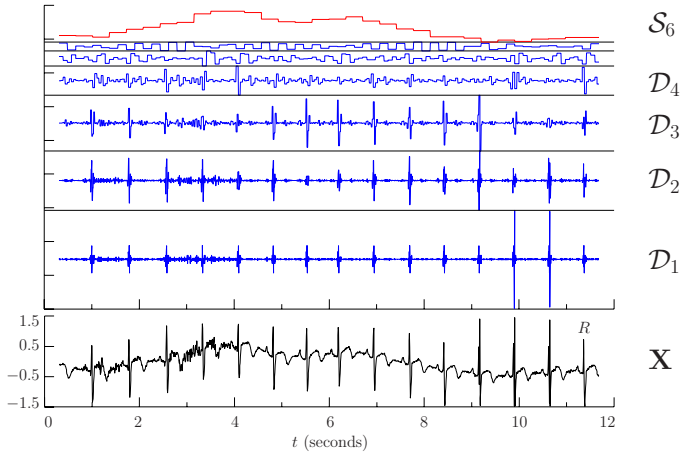

- Haar DWT multiresolution analysis of ECG time series
- blocky nature of Haar basis vectors readily apparent

Electrocardiogram Data: X

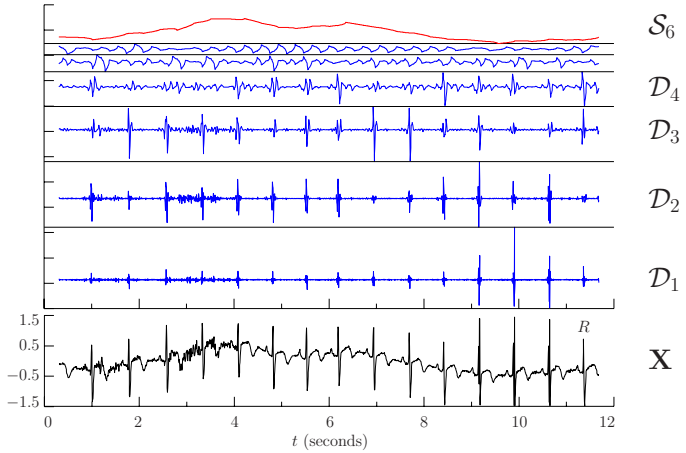

- D(4) DWT multiresolution analysis
- 'shark's fin' evident in $\mathcal{D}_5$ and $\mathcal{D}_6$

Electrocardiogram Data: XI

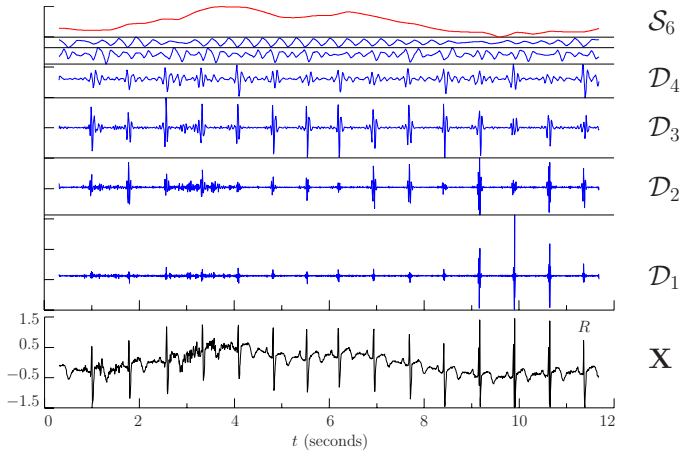

- LA(8) DWT MRA (shape of filter less prominent here)
- note where features end up (will find MODWT does better)

Effect of Circular Shifts on DWT: I

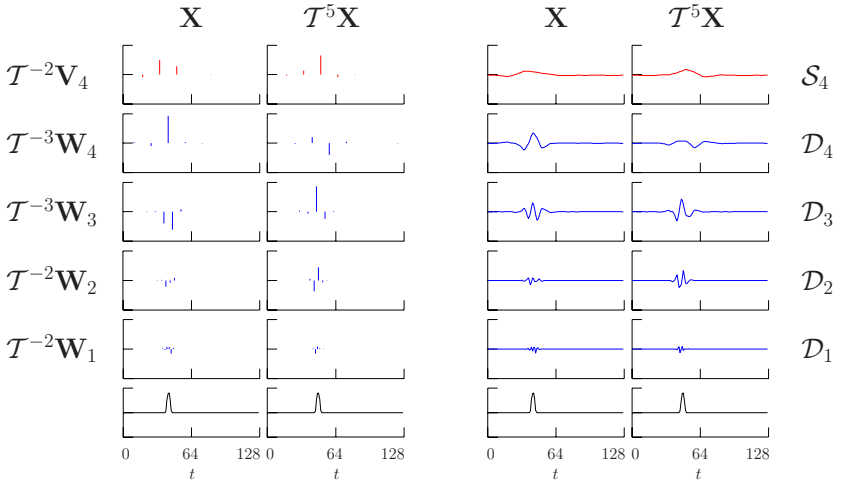

- bottom row: bump $\mathbf{X}$ and bump shifted to right by 5 units
- $J_0 = 4$ LA(8) DWTs (first 2 columns) and MRAs (last 2)

Effect of Circular Shifts on DWT: II

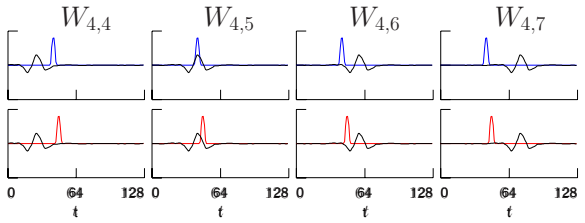

- level $J_0 = 4$ basis vectors used in LA(8) DWT to produce wavelet coefficients $W_{4,j}$, $j = 4, \ldots, 7$ (black curves)
- 'bump' time series $\mathbf{X}$ (blue curves in top row of plots)
- shifted bump series $\mathcal{T}^5\mathbf{X}$ (red curves, bottom row)
- inner product between plotted basis vector and time series yields labeled wavelet coefficient
- alignment between basis vectors and time series explains why DWTs for two series are quite different

Effect of Circular Shifts on MODWT

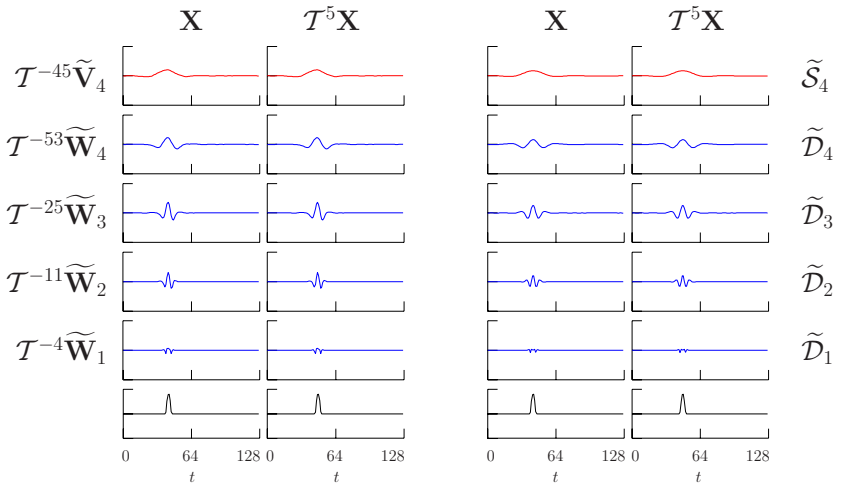

- unlike the DWT, shifting a time series shifts the MODWT coefficients and components of MRA

Electrocardiogram Data: XII

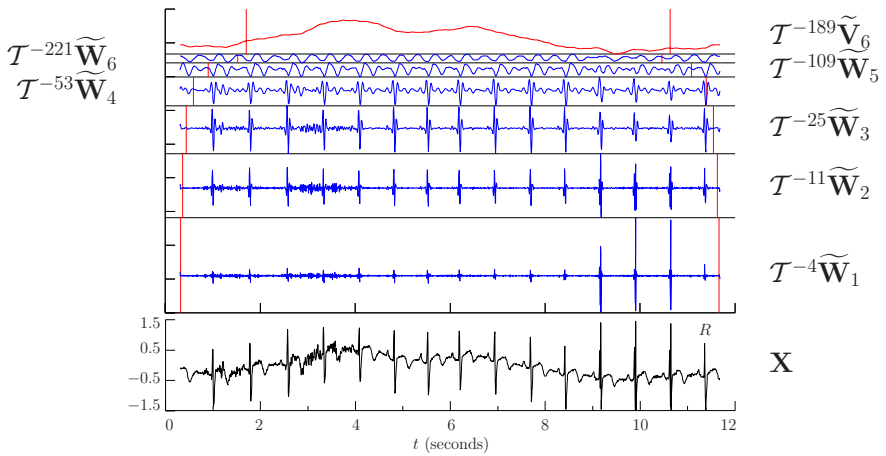

- level $J_0 = 6$ LA(8) MODWT, with $\widetilde{\mathbf{W}}_j$'s circularly shifted
- vertical lines delineate 'boundary' coefficients (explained later)

Electrocardiogram Data: XIII

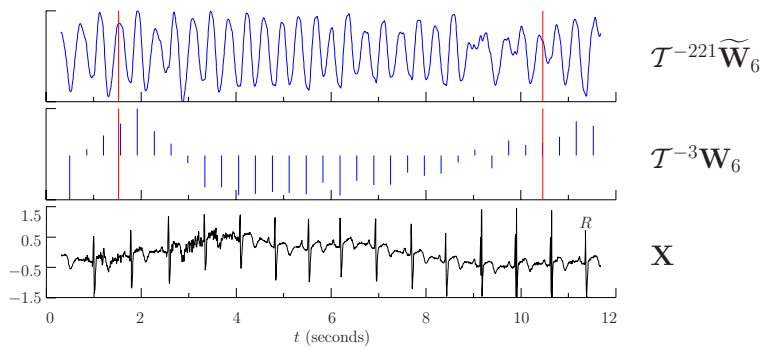

- comparison of level 6 MODWT and DWT wavelet coefficients, after shifting for time alignment
- boundary coefficients delineated by vertical red lines
- subsampling & rescaling $\widetilde{\mathbf{W}}_6$ yields $\mathbf{W}_6$ (note 'aliasing' effect)

Electrocardiogram Data: XIV

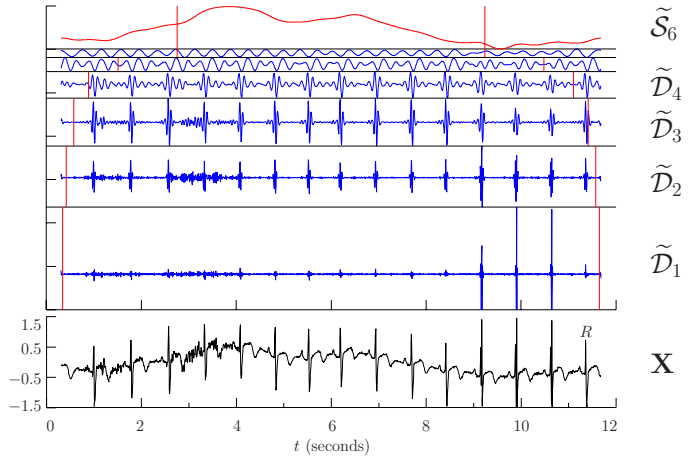

- LA(8) MODWT multiresolution analysis of ECG data

Electrocardiogram Data: XV

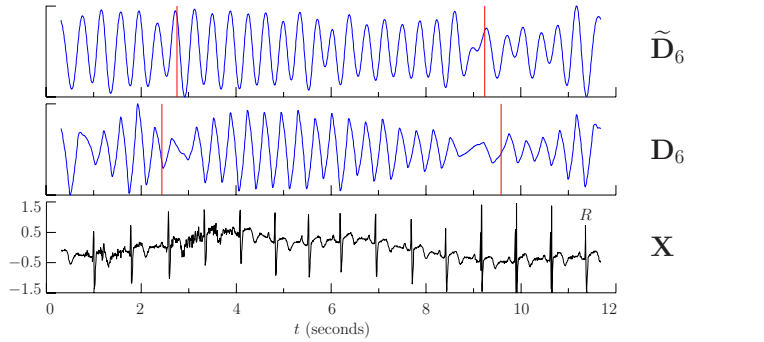

- MODWT details seem more consistent across time than DWT details; e.g., $\widetilde{\mathcal{D}}_6$ does not fade in and out as much as $\mathcal{D}_6$
- 'bumps' in $\mathcal{D}_6$ are slightly asymmetric, whereas those in $\widetilde{\mathcal{D}}_6$ aren't

Electrocardiogram Data: XVI

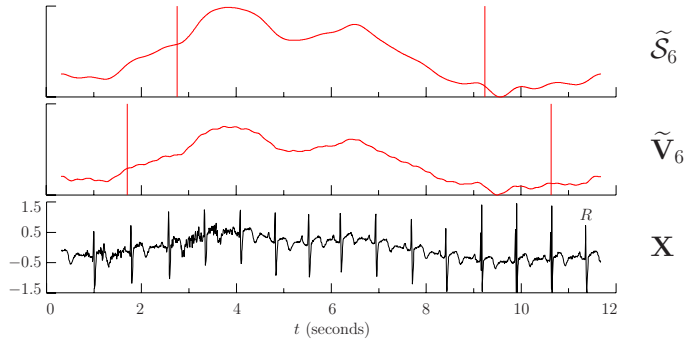

- MODWT coefficients and MRA resemble each other, with latter being necessarily smoother due to second round of filtering
- in the above, $\widetilde{\mathcal{S}}_6$ is somewhat smoother than $\widetilde{\mathbf{V}}_6$ and is an intuitively reasonable estimate of the baseline drift

Subtidal Sea Level Fluctuations: I

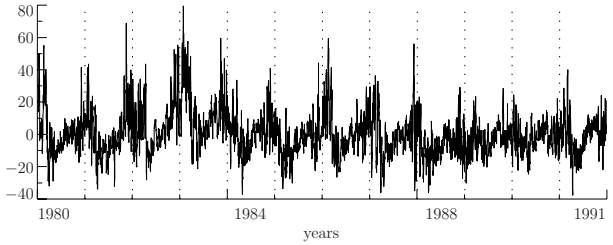

$\mathbf{X}$

- subtidal sea level fluctuations $\mathbf{X}$ for Crescent City, CA, collected by National Ocean Service with permanent tidal gauge
- $N = 8746$ values from Jan 1980 to Dec 1991 (almost 12 years)
- one value every 12 hours, so $\Delta t = 1/2$ day
- 'subtidal' is what remains after diurnal & semidiurnal tides are removed by low-pass filter (filter seriously distorts frequency band corresponding to first physical scale $\tau_1 \, \Delta t = 1/2$ day)

Subtidal Sea Level Fluctuations: II

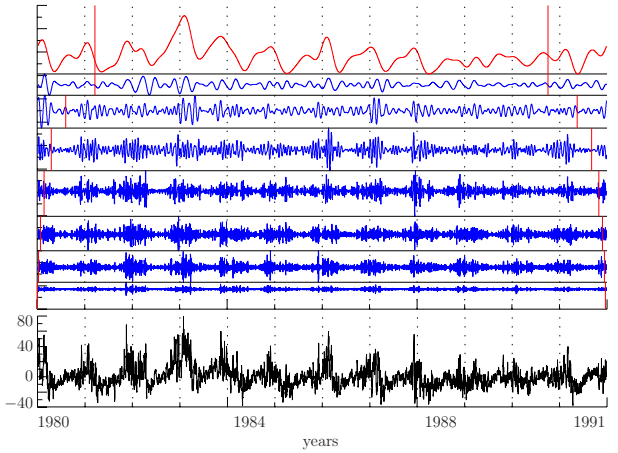

- level $J_0 = 7$ LA(8) MODWT multiresolution analysis

Subtidal Sea Level Fluctuations: III

- LA(8) picked in part to help with time alignment of wavelet coefficients, but MRAs for D(4) and C(6) are OK
- Haar MRA suffers from 'leakage'
- with $J_0 = 7$, $\widetilde{\mathcal{S}}_7$ represents averages over scale $\lambda_7 \, \Delta t = 64$ days
- this choice of J_0 captures intra-annual variations in $\widetilde{\mathcal{S}}_7$ (not of interest to decompose these variations further)

Subtidal Sea Level Fluctuations: IV

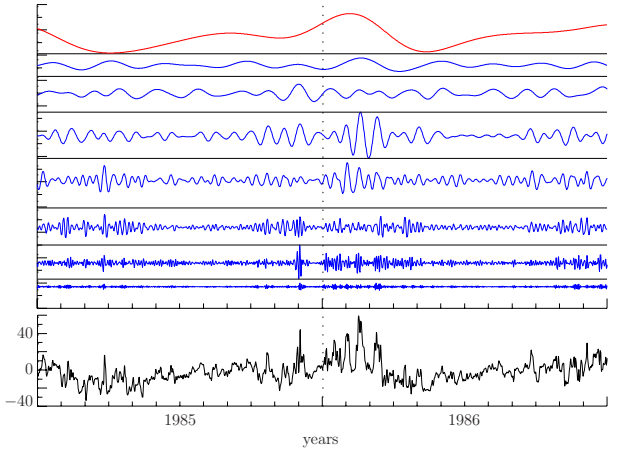

- expanded view of 1985 and 1986 portion of MRA
- lull in $\widetilde{\mathcal{D}}_2$, $\widetilde{\mathcal{D}}_3$ and $\widetilde{\mathcal{D}}_4$ in December 1985 (associated with changes on scales of 1, 2 and 4 days)

Subtidal Sea Level Fluctuations: V

- MRA suggests seasonally dependent variability at some scales
- because MODWT-based MRA does not preserve energy, preferable to study variability via MODWT wavelet coefficients
- cumulative variance plots for $\widetilde{\mathbf{W}}_j$ useful tool for studying time dependent variance
- can create these plots for LA or coiflet-based $\widetilde{\mathbf{W}}_j$ as follows
- form $\mathcal{T}^{-|\nu_j^{(H)}|}\widetilde{\mathbf{W}}_j$, i.e., circularly shift $\widetilde{\mathbf{W}}_j$ to align with $\mathbf{X}$

Subtidal Sea Level Fluctuations: VI

- form normalized cumulative sum of squares:

$$C_{j,t} \equiv \frac{1}{N}\sum_{u=0}^{t} \widetilde{W}^2_{j,u+|\nu_j^{(H)}| \bmod N}, \quad t = 0, \ldots, N-1;$$

  note that $C_{j,N-1} = \|\mathcal{T}^{-|\nu_j^{(H)}|}\widetilde{\mathbf{W}}_j\|^2/N = \|\widetilde{\mathbf{W}}_j\|^2/N$
- examples for $j = 2$ (left-hand plot) and $j = 7$ (right-hand)

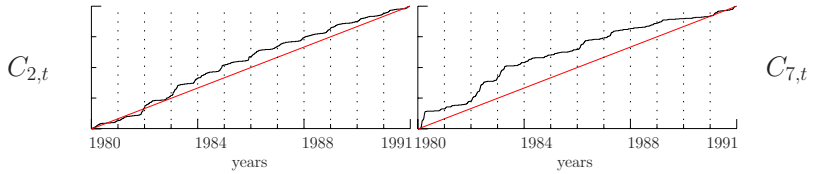

Subtidal Sea Level Fluctuations: VII

- easier to see how variance is building up by subtracting uniform rate of accumulation $tC_{j,N-1}/(N-1)$ from $C_{j,t}$:

$$C'_{j,t} \equiv C_{j,t} - t\frac{C_{j,N-1}}{N-1}$$

- yields rotated cumulative variance plots

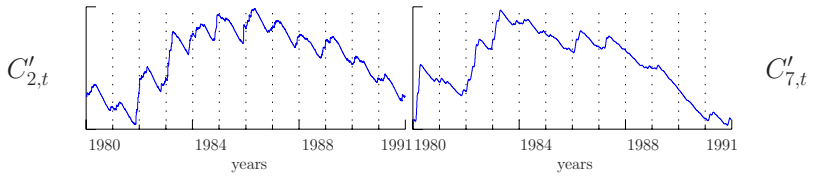

- $C'_{2,t}$ and $C'_{7,t}$ associated with physical scales of 1 and 32 days
- helps build up picture of how variability changes within a year

Subtidal Sea Level Fluctuations: VIII

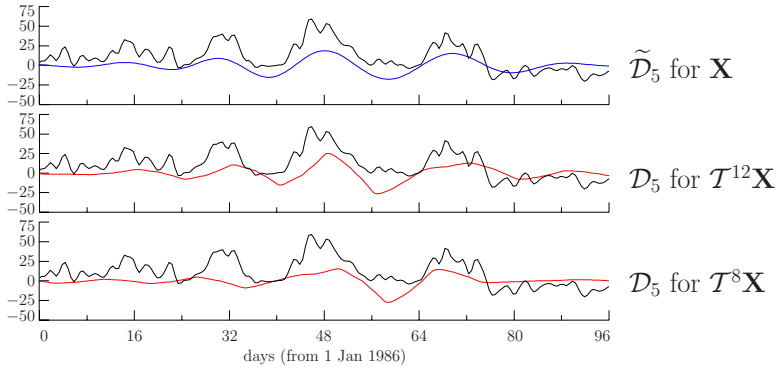

- comparison of alignment properties of DWT and MODWT details $\mathcal{D}_5$ and $\widetilde{\mathcal{D}}_5$, both associated with changes on a physical scale of $\tau_5\,\Delta t = 8$ days (distance between tick marks)
- DWT details evidently suffer from alignment effects

Nile River Minima: I

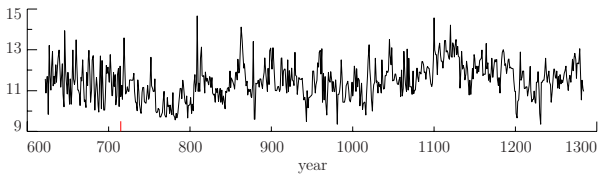

- time series $\mathbf{X}$ of minimum yearly water level of the Nile River
- data from 622 to 1284, but actually extends up to 1921
- data after about 715 recorded at the Roda gauge near Cairo
- method(s) used to record data before 715 source of speculation
- oldest time series actually recorded by humans?!

Nile River Minima: II

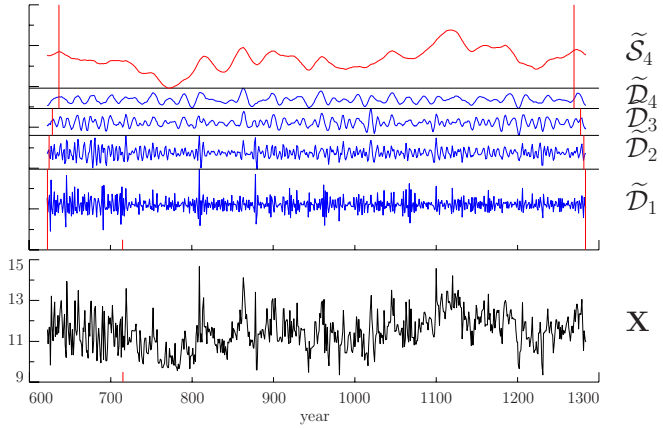

- level $J_0 = 4$ Haar MODWT MRA points out enhanced variability before 715 at scales $\tau_1 \Delta t = 1$ year and $\tau_2 \Delta t = 2$ year
- Haar wavelet adequate (minimizes # of boundary coefficients)

Ocean Shear Measurements: I

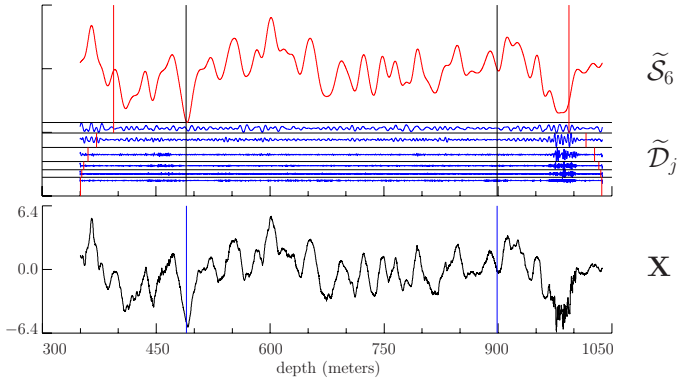

- level $J_0 = 6$ MODWT multiresolution analysis using LA(8) wavelet of vertical shear measurements (in inverse seconds) versus depth (in meters; series collected & supplied by Mike Gregg, Applied Physics Laboratory, University of Washington)

Ocean Shear Measurements: II

- $\Delta t = 0.1$ meters and $N = 6875$
- LA(8) protects against leakage and permits coefficients to be aligned with depth
- $J_0 = 6$ yields smooth $\widetilde{\mathcal{S}}_6$ that is free of bursts (these are isolated in the details $\widetilde{\mathcal{D}}_j$)
- note small distortions at beginning/end of $\widetilde{\mathcal{S}}_6$ evidently due to assumption of circularity
- vertical blue lines delineate subseries of 4096 'burst free' values (to be reconsidered later)
- since MRA is dominated by $\widetilde{\mathcal{S}}_6$, let's focus on details alone

Ocean Shear Measurements: III

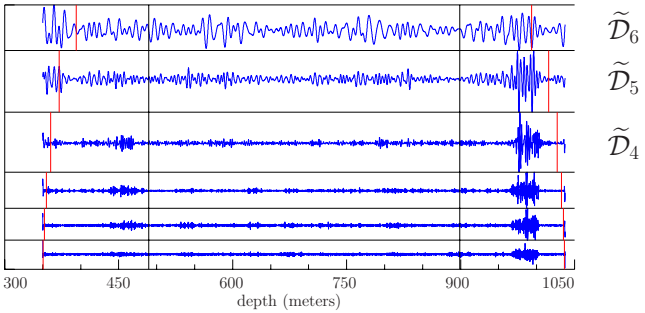

- $\widetilde{\mathcal{D}}_j$'s pick out bursts around 450 and 975 meters, but two bursts have somewhat different characteristics
- possible physical interpretation for first burst: turbulence in $\widetilde{\mathcal{D}}_4$ drives shorter scale turbulence at greater depths
- hints of increased variability in $\widetilde{\mathcal{D}}_5$ and $\widetilde{\mathcal{D}}_6$ prior to second burst

Choice of Wavelet Filter: I

- basic strategy: pick wavelet filter with smallest width L that yields an acceptable analysis (smaller L means fewer boundary coefficients)
- very much application dependent
  - LA(8) good choice for MRA of ECG data and for time/depth dependent analysis of variance (ANOVA) of subtidal sea levels and shear data
  - D(4) or LA(8) good choice for MRA of subtidal sea levels, but Haar isn't (details 'locked' together, i.e., are not isolating different aspects of the data)
  - Haar good choice for MRA of Nile River minima

Choice of Wavelet Filter: II

- can often pick L via simple procedure of comparing different MRAs or ANOVAs (this will sometimes rule out Haar if it differs too much from D(4), D(6) or LA(8) analyses)
- for MRAs, might argue that we should pick $\{h_l\}$ that is a good match to the 'characteristic features' in $\mathbf{X}$
  - hard to quantify what this means, particularly for time series with different features over different times and scales
  - Haar and D(4) are often a poor match, while the LA filters are usually better because of their symmetry properties
  - can use NPESs to quantify match between $\{h_l\}$ and $\mathbf{X}$
- use LA filters if time alignment of $\{W_{j,t}\}$ with $\mathbf{X}$ is important (LA filters with even $L/2$, i.e., 8, 12, 16 or 20, yield better alignment than those with odd $L/2$)

Choice of Level J_0: I

- again, very much application dependent, but often there is a clear choice
  - $J_0 = 6$ picked for ECG data because it isolated the baseline drift into $\mathbf{V}_6$ and $\widetilde{\mathbf{V}}_6$, and decomposing this drift further is of no interest in studying heart rhythms
  - $J_0 = 7$ picked for subtidal sea levels because it trapped intra-annual variations in $\widetilde{\mathbf{V}}_7$ (not of interest to analyze these)
  - $J_0 = 6$ picked for shear data because $\widetilde{\mathbf{V}}_6$ is free of bursts; i.e., $\widetilde{\mathbf{V}}_{J_0}$ for $J_0 < 6$ would contain a portion of the bursts
  - $J_0 = 4$ picked for Nile River minima to demonstrate that its time-dependent variance is due to variations on the two smallest scales

Choice of Level J_0: II

- as J_0 increases, there are more boundary coefficients to deal with, which suggests not making J_0 too big
- if application doesn't naturally suggest what J_0 should be, an *ad hoc* (but reasonable) default is to pick J_0 such that circularity assumption influences $< 50\%$ of $\mathbf{W}_{J_0}$ or $\mathcal{D}_{J_0}$ (next topic of discussion)

Handling Boundary Conditions: I

- DWT and MODWT treat time series $\mathbf{X}$ as if it were circular
- circularity says X_{N-1} is useful surrogate for X_{-1} (sometimes this is OK, e.g., subtidal sea levels, but in general it is questionable)
- first step is to delineate which parts of $\mathbf{W}_j$ and $\mathcal{D}_j$ are influenced (at least to some degree) by circular boundary conditions
- by considering

$$W_{j,t} = 2^{j/2}\widetilde{W}_{j,2^j(t+1)-1} \text{ and } \widetilde{W}_{j,t} \equiv \sum_{l=0}^{L_j-1} \tilde{h}_{j,l} X_{t-l \bmod N},$$

can determine that circularity affects

$$W_{j,t},\ t = 0, \ldots, L'_j - 1 \text{ with } L'_j \equiv \left\lceil (L-2)\left(1 - \frac{1}{2^j}\right)\right\rceil$$

Handling Boundary Conditions: II

- can argue that $L'_1 = \frac{L}{2} - 1$ and $L'_j = L - 2$ for large enough j
- circularity also affects the following elements of $\mathcal{D}_j$:

$$t = 0, \ldots, 2^j L'_j - 1 \text{ and } t = N - (L_j - 2^j), \ldots, N-1,$$

where $L_j = (2^j - 1)(L-1) + 1$

- for MODWT, circularity affects

$$\widetilde{W}_{j,t}, \quad t = 0, \ldots, \min\{L_j - 2, N-1\}$$

- circularity also affects the following elements of $\widetilde{\mathcal{D}}_j$:

$$t = 0, \ldots, L_j - 2 \text{ and } t = N - L_j + 1, \ldots, N-1$$

Handling Boundary Conditions: III

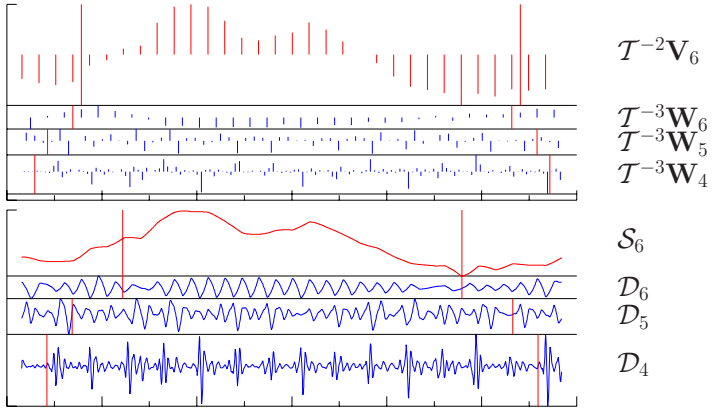

- examples of delineating LA(8) DWT boundary coefficients for ECG data and of marking parts of MRA influenced by circularity

Handling Boundary Conditions: IV

- boundary regions increase as the filter width L increases
- for fixed L, boundary regions in DWT MRAs are smaller than those for MODWT MRAs
- for fixed L, MRA boundary regions increase as J_0 increases (an exception is the Haar DWT)
- these considerations might influence our choice of L and DWT versus MODWT

Handling Boundary Conditions: V

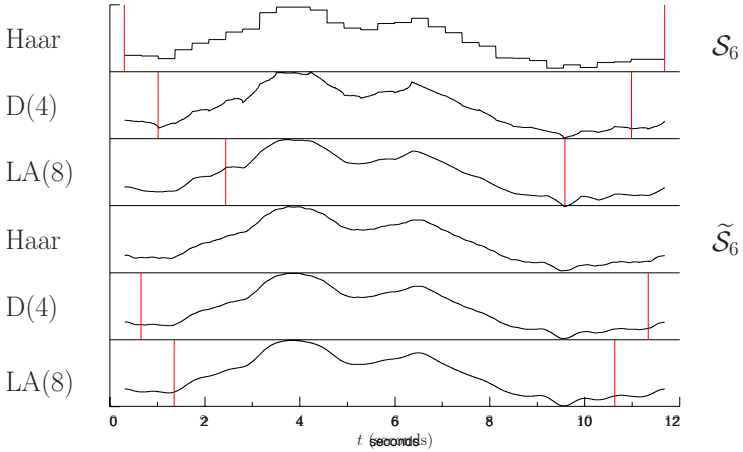

- comparison of DWT smooths $\mathcal{S}_6$ (top 3 plots) and MODWT smooths $\widetilde{\mathcal{S}}_6$ (bottom 3) for ECG data using, from top to bottom within each group, the Haar, D(4) and LA(8) wavelets

Handling Boundary Conditions: VI

- just delineating parts of $\mathbf{W}_j$ and $\mathcal{D}_j$ that are influenced by circular boundary conditions can be misleading (too pessimistic)
- effective width $\lambda_j = 2\tau_j = 2^j$ of jth level equivalent filters can be much smaller than actual width $L_j = (2^j - 1)(L - 1) + 1$
- arguably less pessimistic delineations would be to always mark boundaries appropriate for the Haar wavelet (its actual width is the effective width for other filters)

Handling Boundary Conditions: VII

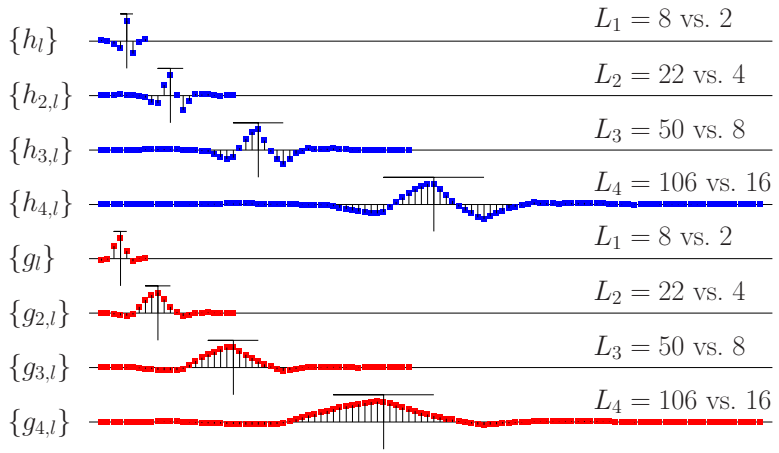

- plots of LA(8) equivalent wavelet/scaling filters, with actual width L_j compared to effective width of 2^j

Handling Boundary Conditions: VIII

- to lessen the impact of boundary conditions, we can use 'tricks' from Fourier analysis, which also treats $\mathbf{X}$ as if it were circular
  - extend series with $\overline{X}$ (similar to zero padding)
  - polynomial extrapolations
  - use 'reflection' boundary conditions by pasting a reflected (time-reversed) version of $\mathbf{X}$ to end of $\mathbf{X}$

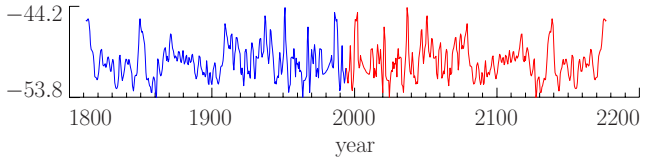

  - note that series so constructed of length $2N$ has same sample mean and sample variance as original series $\mathbf{X}$

Handling Boundary Conditions: IX

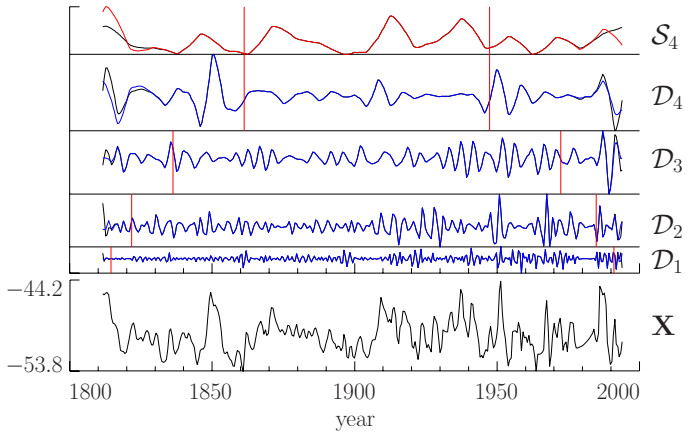

- comparison of effect of reflection (red/blue) and circular (black) boundary conditions on LA(8) DWT-based MRA for oxygen isotope data

Handling Non-Power of Two Sample Sizes

- not a problem with the MODWT, which is defined naturally for all sample sizes N
- partial DWT requires just $N = M2^{J_0}$ rather than $N = 2^J$
- can pad with sample mean $\overline{X}$ etc.
- can truncate down to multiple of 2^{J_0}
  - truncate at beginning of series & do analysis
  - truncate at end of series & do analysis
  - combine two analyses together
- can use a specialized pyramid algorithm involving at most one special term at each level

Lack of Standard Definition for DWT: I

- our definition of DWT matrix $\mathcal{W}$ based upon
  - convolutions rather than inner products
  - odd indexed downsampling rather than even indexed
  - using $(-1)^{l+1}h_{L-1-l}$ to define g_l rather than $(-1)^{l-1}h_{1-l}$
  - ordering coefficients in resulting transform from small to large scale rather than large to small
- choices other than the above are used frequently elsewhere, resulting in DWTs that can differ from what we have presented

Lack of Standard Definition for DWT: II

- two left-hand columns: D(4) DWT matrix $\mathcal{W}$ as defined here
- two right-hand columns: `S-Plus Wavelets` D(4) DWT matrix (after reordering of its row vectors)
- only the scaling coefficient is guaranteed to be the same!!!